

Jet quenching for heavy flavors in AA and pp collisions

B.G. Zakharov¹

¹ *L.D. Landau Institute for Theoretical Physics, GSP-1, 117940,
Kosygina Str. 2, 117334 Moscow, Russia*

We perform a global analysis of experimental data on jet quenching for heavy flavors for scenarios with and without quark-gluon plasma formation in pp collisions. We find that the theoretical predictions for the nuclear modification factor R_{AA} for heavy flavors at the LHC energies are very similar for these scenarios, and the results for R_{AA} and v_2 agree reasonably with the LHC data. The agreement with data at the RHIC top energy becomes somewhat better for the intermediate scenario, in which the quark-gluon plasma formation in pp collisions occurs only at the LHC energies. Our fits to heavy flavor R_{AA} show that description of jet quenching for heavy flavors requires somewhat bigger α_s than data on jet quenching for light hadrons.

PACS numbers:

I. INTRODUCTION

The observed suppression of high- p_T hadron spectra (jet quenching) in nucleus-nucleus (AA) collisions at RHIC and the LHC is one of the main signals of formation of a deconfined quark-gluon plasma (QGP) in the initial stage of AA collisions. Jet quenching in AA collisions is due to radiative [1–6] and collisional [7] energy loss of fast partons traversing the QGP fireball. The dominant contribution to the parton energy loss comes from induced gluon radiation [6, 8]. The suppression of particle spectra in AA collisions as compared to the binary scaled spectra in pp collisions is characterized by the nuclear modification factor R_{AA} . Experimentally, for a centrality class Δc , R_{AA} is defined as

$$R_{AA} = \frac{d^2 N_{AA}/dp_T^2 dy}{N_{ev} \langle T_{AA} \rangle_{\Delta c} d^2 \sigma_{pp}/dp_T^2 dy}, \quad (1)$$

where N_{ev} is the number of events, $d^2 N_{AA}/dp_T^2 dy$ is the particle yield in AA collisions, $\langle T_{AA} \rangle_{\Delta c}$ is the averaged (over the centrality class Δc) nuclear overlap function. The centrality c , which characterizes the overlap of the colliding nuclei, is experimentally determined via charged hadron multiplicity. For heavy ion collisions, to good accuracy the centrality can be written via the impact parameter b as $c \approx \pi b^2 / \sigma_{in}^{AA}$ [9] (except for very peripheral collisions). If one assumes that in proton-proton (pp) collision the QGP is not produced, and the experimental inclusive pp cross section in the denominator of (1) is close to the inclusive pp cross calculated within the pQCD framework, $d^2 \sigma_{pp}^t/dp_T^2 dy$, then the theoretical nuclear modification factor can be written as

$$R_{AA} = \frac{\langle d^2 \sigma_{NN}^m/dp_T^2 dy \rangle_{\Delta c}}{d^2 \sigma_{pp}^t/dp_T^2 dy}, \quad (2)$$

where $d^2 \sigma_{NN}^m/dp_T^2 dy$ is the medium-modified inclusive nucleon-nucleon cross section for a given geometry of the jet production in AA collision, and $\langle \dots \rangle$ means averaging over the jet production geometry and the impact parameter for the centrality bin Δc .

If the QGP formation occurs in pp collisions as well, formula (2) becomes invalid, since in this scenario the pp cross section in the denominator of (1) is affected by the medium effects, and one should use in the denominator of (2) instead of the pQCD pp cross section the one that accounts for jet modification by the final state interaction medium effects in the mini QGP (mQGP). Several signals of the mQGP formation in pp collisions have by now been seen in data on soft hadron production. Among them the observation of the ridge effect [10, 11] in pp collisions at the LHC energies, the steep growth of the strange particle production at $dN_{ch}/d\eta \sim 5$ [12]. The latter fact agrees with the onset of the QGP regime at $dN_{ch}/d\eta \sim 6$ predicted in [13] from experimental data on the mean p_T as a function of multiplicity, employing Van Hove's arguments [14]. From the point of view of the mQGP formation, it is important that in the pp jet events multiplicity of soft (underlying-event (UE)) hadrons is bigger than multiplicity in minimum bias pp collisions by a factor of $\sim 2 - 2.5$ [15]. At the LHC energies $dN_{ch}^{ue}/d\eta \sim 10 - 15$, which turns out to be well above the estimated critical multiplicity density $dN_{ch}/d\eta \sim 5$ for the onset of the mQGP formation

in pp collisions. For pp collisions at the RHIC top energy of $\sqrt{s} = 0.2$ TeV we have $dN_{ch}^{ue}/d\eta \sim 6$, which is of the order of the expected multiplicity for the onset of the QGP formation regime. Thus, it is possible that for pp collisions at $\sqrt{s} \sim 0.2$ TeV the dynamics of the produced soft hadrons may be close to the free streaming regime, and consequently the jet quenching effects should be small. This means that for AA collisions at RHIC the theoretical R_{AA} should be given by the formula (2).

For the scenario with the mQGP production in pp collisions, the real inclusive pp cross section in the denominator of (1) includes the jet quenching effects in the mQGP fireball produced in pp collision. We can write it as the product of the theoretical pQCD pp cross section and the medium modification factor R_{pp}

$$d^2\sigma_{pp}^m/dp_T^2 dy = R_{pp} d^2\sigma_{pp}^{pt}/dp_T^2 dy. \quad (3)$$

Physically, the $d^2\sigma_{pp}^m/dp_T^2 dy$ is similar to the effective NN cross section entering the nominator of (2), but, contrary to (2), now we should perform calculations for the mQGP fireball and perform averaging over the geometry of pp collisions. Thus, in the scenario with the mQGP production in pp collisions the theoretical R_{AA} , as compared to the formula (2), turns out to be enhanced by the factor $1/R_{pp}$. Of course, R_{pp} is not directly observable quantity. Since the size and the temperature of the mQGP fireball in pp collisions should be small, one can expect that the quenching effects should be small, i.e. R_{pp} should be close to unity. This makes it practically impossible the observation of jet quenching in pp collisions via experimental data on the p_T -dependence of hadron spectra. In [16] it was shown that measurement of variation of the photon/hadron-tagged jet fragmentation functions (FFs), characterized by the medium modification factor I_{pp} , with the UE multiplicity may be a promising method for direct observation of the jet quenching in pp collisions. Recently, the ALICE Collaboration reported preliminary results [17] on the medium modification factor I_{pp} at $\sqrt{s} = 5.02$ TeV for the hadron-tagged jets (with the trigger hadron momentum $8 < p_T < 15$ GeV, and the associated away side hadron momentum in the range $4 < p_T < 6$ GeV), that show a monotonic decrease of I_{pp} with the UE multiplicity by about 15-20% for the UE multiplicity density range $\sim 4 - 15$. In [18] it has been shown that this agrees reasonably with theoretical predictions obtained within the light cone path integral (LCPI) [2] approach to induced gluon emission. The observation of the decrease of I_{pp} with the UE multiplicity, if confirmed, will be a strong argument for the scenario with the mQGP production in pp jet events.

In the light of the possibility of the mQGP formation in pp collisions, it is of great interest to perform analysis of jet quenching in AA collisions for such a scenario. In [19], we have performed the global analysis of the data on jet quenching in AA collisions for light hadrons for scenarios with and without the mQGP production in pp collisions within the LCPI approach [2] to induced gluon emission. We used $\alpha_s(Q, T)$ which has a plateau around $Q \sim Q_{fr} = \kappa T$ (this form is motivated by the lattice results for the in-medium QCD coupling [20] and calculations within the functional renormalization group [21]). We fitted κ using the LHC heavy ion data on the nuclear modification factor R_{AA} in 2.76 and 5.02 TeV Pb+Pb, and 5.44 TeV Xe+Xe collisions. Calculations in this way allow to avoid the ambiguities in the choice of α_s for small systems, because the parameter κ , fitted to data for heavy ion collisions, automatically fixes α_s for small size QGP. In [19] it was found that both the models lead to quite good description of the RHIC and the LHC data on R_{AA} for heavy ion collisions. For the RHIC PHENIX data on R_{AA} the agreement becomes somewhat better for a scenario when the mQGP formation in pp collisions occurs at the LHC energies, but is absent for the RHIC energies.

It would be interesting to examine whether the scenario with the mQGP formation in pp collisions is consistent with the data on jet quenching for heavy flavors as well. Jet quenching for heavy flavors has attracted much theoretical and experimental attention in recent years (for recent review, see [22]). Initially it was expected that heavy quarks should lose less energy than light quarks due to the dead cone suppression of the radiative energy loss for heavy quarks [23]. However, later experiments at RHIC [24, 25] observed a quite strong suppression of single electrons from decays of heavy mesons that seemed to be in contradiction with expected dead cone suppression of the radiative energy loss (the ‘‘heavy quark puzzle’’). On the theoretical side, in [26] within the LCPI approach [2] to the induced gluon emission it was found that, due to the quantum finite-size effects (ignored in the dead cone model [23]), at low energies ($\lesssim 20 - 30$ GeV) the quark mass suppression of radiative energy loss turns out to be significantly smaller than predicted in the dead cone model. Moreover, at energies $\gtrsim 100$ GeV the quantum effects lead to an increase of the radiative energy loss with the quark mass. In Refs. [27, 28] we analyzed the first data on jet quenching for heavy flavors from the LHC within the LCPI approach for the scenario without the mQGP production in pp collisions, and found a reasonable agreement with the data. To

date, a substantial amount of experimental data on jet quenching for heavy flavors has been obtained at the LHC. This allows to perform a more detailed comparison of theory and experiment for the heavy flavor jet quenching. In the context of the heavy quark puzzle, it is important that the scenario with the mQGP formation can lead to some reduction of the heavy-to-light ratios of the nuclear modification factors R_{AA} [29]. This occurs due to the flavor hierarchy $R_{pp}^\pi < R_{pp}^D < R_{pp}^B$ [29], which is valid at $p_T \lesssim 20$ GeV for the RHIC energy $\sqrt{s} = 0.2$ TeV and at $p_T \lesssim 70$ GeV for the LHC energies [29].

In this paper we extend the analysis of [19] of jet quenching for light hadrons to heavy mesons and heavy flavor electrons (HFEs). As in [19], we calculate the induced gluon emission x -spectrum, dP/dx (x is the gluon fractional momentum), within the LCPI approach [2] (see also [30] for a more recent discussion of the LCPI formalism). In this approach dP/dx is expressed through the solution of a two-dimensional Schrödinger equation, which automatically accounts for all rescatterings of fast partons in the medium. We calculate the induced gluon spectrum using the form suggested in [31]¹. We calculate the induced gluon spectrum beyond the soft gluon approximation. In the literature the heavy quark energy loss is usually calculated in the soft gluon approximation (see e.g. [32–38]). However, one can easily show that this approximation is too crude for analysis of the quark mass effects. Indeed, in the two-dimensional Schrödinger equation, which defines the induced gluon x -spectrum, the quark mass enters only through the formation length $L_f = 2x(1-x)E/[m_q^2x^2 + m_g^2(1-x)]$ [2] (here E is the initial quark energy, $m_{q,g}$ are the quasiparticle parton masses). For this reason, the quark mass becomes important at $x^2/(1-x) \gtrsim m_g^2/m_q^2$. Taking $m_g \sim 400$ MeV [39], one can see that for $c(b)$ -quark it occurs at $x \gtrsim 0.3(0.1)$ (accurate computations of [26] corroborate these qualitative estimates). This says that the soft gluon approximation may be unsatisfactory for heavy flavors (especially for c -quark). Note also that our scheme treats accurately the Coulomb effects in parton rescatterings (contrary to available in the literature [34–36] perturbative treatment of the Coulomb effects as a correction to the harmonic oscillator approximation), that are very important for the quark mass effects [26].

The plan of the paper is as follows. In section 2, we briefly review the basic aspects of our model. In section 3 we present results for R_{pp} and comparison of our results with experimental data on R_{AA} and on the elliptic flow coefficient v_2 in AA collisions. Section 4 presents a summary.

II. OUTLINE OF THE JET QUENCHING MODEL

We use the jet quenching scheme of [40] in the form of [41] with a somewhat improved treatment of multiple gluon emission and adopted for use of a T -dependent α_s (as in [19]). In this section we briefly discuss the basic features of our theoretical scheme. More details can be found in Refs. [19, 40, 41].

For a given geometry of the AA collision and of the jet production we write the medium-modified hard cross section for NN collision in a form similar to the ordinary pQCD formula for NN collisions in vacuum

$$\frac{d\sigma^m(N + N \rightarrow h + X)}{d\mathbf{p}_T dy} = \sum_i \int_0^1 \frac{dz}{z^2} D_{h/i}^m(z, Q) \frac{d\sigma^{pt}(N + N \rightarrow i + X)}{d\mathbf{p}_T^i dy}, \quad (4)$$

where $d\sigma^{pt}(N + N \rightarrow i + X)/d\mathbf{p}_T^i dy$ is the standard pQCD hard cross section for production of the initial hard parton i with the transverse momentum $\mathbf{p}_T^i = \mathbf{p}_T/z$, $D_{h/i}^m$ is the medium-modified FF describing the production of the observed particle h from the fragmentation of the initial hard parton i . For the initial virtuality scale Q we use the parton momentum p_T^i . We calculate hard cross sections using the LO pQCD formula with the CTEQ6 [42] parton distribution functions. The nuclear modification of the parton distribution functions for AA collisions are accounted with the EPS09 correction [43] (this correction gives a small deviation of R_{AA} from unity even without the jet quenching effects). To simulate the higher order effects, as in the PYTHIA event generator [44], we calculate α_s for the virtuality scale cQ with $c = 0.265$. This gives a fairly good description of the p_T -dependence of the particle spectra for pp collisions (note that the normalization of hard cross sections is not important for R_{AA} at all).

¹ Contrary to the original LCPI form of the induced gluon spectrum in terms of the singular Green functions [2], the method of [31] reduces calculation of the gluon spectrum to solving an initial boundary value problem with a smooth initial condition, which is convenient for numerical calculations.

We assume that the induced gluon emission stage occurs after the DGLAP one (this approximation is reasonable since the formation length for the leading DGLAP gluon emission is rather small [40]), and that formation of the final particle h occurs outside the QGP fireball. In this picture, the medium-modified FF for $i \rightarrow h$ transition can be written as

$$D_{h/i}^m(Q) \approx D_{h/j}(Q_0) \otimes D_{j/k}^{in} \otimes D_{k/i}(Q), \quad (5)$$

where \otimes means z -convolution, $D_{k/i}$ is the DGLAP FF for $i \rightarrow k$ parton transition, $D_{j/k}^{in}$ is the FF for $j \rightarrow k$ in-medium parton transition in the QGP fireball, and $D_{h/j}$ describes the vacuum fragmentation of the parton j into the final particle h outside of the QGP. We computed the DGLAP FFs using the PYTHIA event generator [44].

For the FFs of the heavy quarks for $c \rightarrow D$ and $b \rightarrow B$ transitions we use the Peterson parametrization

$$D_{M/Q}(z) \propto \frac{1}{z[1 - (1/z) - \epsilon_Q/(1-z)]^2} \quad (6)$$

with $\epsilon_c = 0.06$ and $\epsilon_b = 0.006$. As in [28], for HFEs we write the electron z -distribution for $Q \rightarrow e$ transition as a convolution $D_{e/Q} = D_{e/M} \otimes D_{M/Q}$. We express $D_{e/M}$ for the $M \rightarrow e$ decays² via the electron momentum spectrum dB/dp in the heavy meson rest frame

$$D_{e/M}(z, P) = \frac{P}{4} \int_0^\infty dq^2 \frac{\cosh(\phi - \theta)}{p^2 \cosh \phi} \cdot \frac{dB}{dp}, \quad (7)$$

where $p = \sqrt{(q^2 + m_e^2) \cosh^2(\phi - \theta) - m_e^2}$, $\theta = \text{arcsinh}(P/M)$, $\phi = \text{arcsinh}(zP/\sqrt{q^2 + m_e^2})$, P is the heavy meson momentum, and M is its mass. For dB/dp in the B/D -meson decays we use the CLEO data [46, 47] on the electron spectra. We calculate the z -distribution of the nonprompt D mesons from beauty-hadron decays, $D_{D/B}(z, P)$, using a form similar to (7) (with replacement $m_e \rightarrow m_D$) with the D meson spectrum dB/dp obtained by the BaBar Collaboration [48].

For numerical calculation of the one gluon emission spectrum dP/dx we use the representation derived in [31]. For the convenience of the reader formulas for calculation of dP/dx are given in Appendix. For heavy quark masses we take $m_c = 1.2$ GeV and $m_b = 4.75$ GeV. For the gluon quasiparticle mass we take $m_g = 400$ MeV [39] (as in [19], for jet quenching of light hadrons). As in [19], we calculate the dipole cross section, which is necessary for calculation of the imaginary potential (14) in the Schrödinger equation for calculation of dP/dx , using the Debye mass from the lattice simulations of [49].

We calculate the FFs $D_{j/k}^{in}$ for heavy quarks via the one gluon spectrum dP/dx in the approximation of the independent multiple gluon emission [50] in the same way as in our previous jet quenching analyses for light hadrons (see Appendix B of [41] for details). As in [19, 40], we treat the collisional mechanism as a perturbation to the radiative one by redefining the initial QGP temperature in calculating the radiative medium-modified FFs $D_{j/k}^{in}$. We calculate the collisional energy loss using the Bjorken method [7] with an accurate treatment of kinematics of the $2 \rightarrow 2$ processes (the details can be found in [8]).

As in [19], we take $\alpha_s(Q, T)$ in the form

$$\alpha_s(Q, T) = \begin{cases} \frac{4\pi}{9 \log(Q^2/\Lambda_{QCD}^2)} & \text{if } Q > Q_{fr}(T), \\ \alpha_s^{fr}(T) & \text{if } Q_{fr}(T) \geq Q \geq cQ_{fr}(T), \\ \alpha_s^{fr}(T) \times (Q/cQ_{fr}(T)) & \text{if } Q < cQ_{fr}(T), \end{cases} \quad (8)$$

where $Q_{fr} = \Lambda_{QCD} \exp\{2\pi/9\alpha_s^{fr}\}$ (in the present analysis we take $\Lambda_{QCD} = 200$ MeV), $c = 0.8$. We take $Q_{fr} = \kappa T$, and perform fit of the free parameter κ using data on the nuclear modification factor R_{AA} for heavy ion collisions. The form (8) is supported by the lattice results [20] for the in-medium α_s .

We use the same model of the QGP fireball as in [19] with Bjorken's 1+1D expansion of the QGP [51] (that leads to the entropy density $s(\tau)/s(\tau_0) = \tau_0/\tau$ with τ_0 the thermalization time) and a flat

² Note that we ignore the $B \rightarrow D \rightarrow e$ process since it gives a negligible contribution [45].

entropy profile in the the transverse coordinates. We take $\tau_0 = 0.5$ fm. We use a linear parametrization $s(\tau) = s(\tau_0)\tau/\tau_0$ for $\tau < \tau_0$. To fix $s(\tau_0)$ in AA collisions we use the predictions of the Glauber wounded nucleon model [52] with parameters obtained in our Monte-Carlo Glauber analyses [53, 54] by fitting data on the charged hadron multiplicity pseudorapidity density $dN_{ch}/d\eta$ in AA collisions from RHIC (for 0.2 TeV Au+Au collisions) and the LHC (for 2.76 and 5.02 TeV Pb+Pb collisions). For the entropy/multiplicity ratio we take $dS/dy/dN_{ch}/d\eta \approx 7.67$ [55]. Our Glauber model gives for the initial QGP temperature (for the ideal gas QGP with $N_f = 2.5$) $T_0 \approx 320$ MeV for central Au+Au collisions at $\sqrt{s} = 0.2$ TeV, and $T_0 \approx 400(420)$ MeV for central Pb+Pb collisions at $\sqrt{s} = 2.76(5.02)$ TeV (see Fig. 1 in [19]). As in [19], we transform the almond shaped overlap region of two colliding nuclei into an elliptic one (of the same area), which reproduces the fireball eccentricity ϵ_2 obtained within our Monte-Carlo Glauber model. Note that for the Monte-Carlo version of the Glauber model ϵ_2 does not vanish for central collisions (due to density fluctuations), contrary to the optical Glauber model. This fact is practically irrelevant for R_{AA} , but is important for predictions of the azimuthal anisotropy v_2 (see discussion in [19]).

As in [19], for mQGP produced in pp collisions we use the model of an effective fireball (that includes pp collisions with all impact parameters). In this picture, using the data on the UE charged multiplicity density $dN_{ch}^{ue}/d\eta$, we obtain for the radius and the initial temperature T_0 of the mQGP fireball produced in pp collisions [19]

$$R_f[\sqrt{s} = 0.2, 2.76, 5.02 \text{ TeV}] \approx [1.26, 1.44, 1.49] \text{ fm}, \quad (9)$$

$$T_0[\sqrt{s} = 0.2, 2.76, 5.02 \text{ TeV}] \approx [195(226), 217(247), 226(256)] \text{ MeV}. \quad (10)$$

In (10) we present T_0 for the ideal gas entropy and for the lattice entropy [56] (numbers in brackets).

For pp collisions we calculate the medium-modified hard cross sections in the same way as for AA collisions. We calculate the L -distribution of the jet path lengths in the mQGP fireball using the distribution of the jet production points for the MIT bag model quark density (assuming the same density for quarks and gluons).

III. COMPARISON WITH EXPERIMENTAL DATA

In this section we compare the model predictions with data for the nuclear modification factor R_{AA} and the azimuthal anisotropy v_2 for heavy mesons and HFEs. We present results for two sets of the optimal values of the free parameter κ in the parametrization (8) of α_s . The first set (for the versions with and without mQGP formation in pp collisions) of the optimal values of κ have been obtained by the χ^2 fitting data from the LHC on R_{AA} for D mesons [57–60] and HFEs [61, 62] in 2.76 and 5.02 TeV Pb+Pb collisions with centralities $\lesssim 50\%$. We used data points with $p_T \gtrsim 10$ GeV for D mesons, and $p_T \gtrsim 5$ GeV for HFEs³. The fits of the heavy flavor data give $\kappa \approx 2(1.4)$ for the versions without(with) the mQGP formation in pp collisions (in the following we denote them as $\kappa_H(\kappa_H^{mQGP})$). For the optimal values $\kappa_H(\kappa_H^{mQGP})$ we obtained in these fits $\chi^2/d.p. \approx 0.69(0.71)$ (χ^2 per data point). For the second set we use the values of κ obtained in [19] by fitting the LHC data on R_{AA} for charged hadrons for 2.76 and 5.02 TeV Pb+Pb collisions, and 5.44 TeV Xe+Xe collisions. These fits give $\kappa \approx 3.4(2.5)$ for the scenarios without(with) the mQGP production in pp collisions (in the following we denote them as $\kappa_L(\kappa_L^{mQGP})$). For the optimal values $\kappa_L(\kappa_L^{mQGP})$, obtained by fitting R_{AA} for charged hadrons, we have for the heavy flavor data the values $\chi^2/d.p. \approx 1.95(1.45)$, that show that $\kappa_L(\kappa_L^{mQGP})$ also lead to reasonable agreement with the heavy flavor experimental data.

In Fig. 1 we show the results for R_{pp} obtained for the optimal value $\kappa = \kappa_H^{mQGP}$ (upper panels) and $\kappa = \kappa_L^{mQGP}$ (lower panels) for $\sqrt{s} = 0.2$, $\sqrt{s} = 2.76$, and 5.02 TeV. To demonstrate the difference between

³ For HFEs we use a smaller lower limit of p_T since for HFEs, due to the presence of the additional FF $D_{e/M}$, the ratio of the typical transverse momentum of the original heavy quarks to the transverse momentum of the final detected particle for HFEs becomes bigger by a factor of ~ 2 than that for heavy mesons.

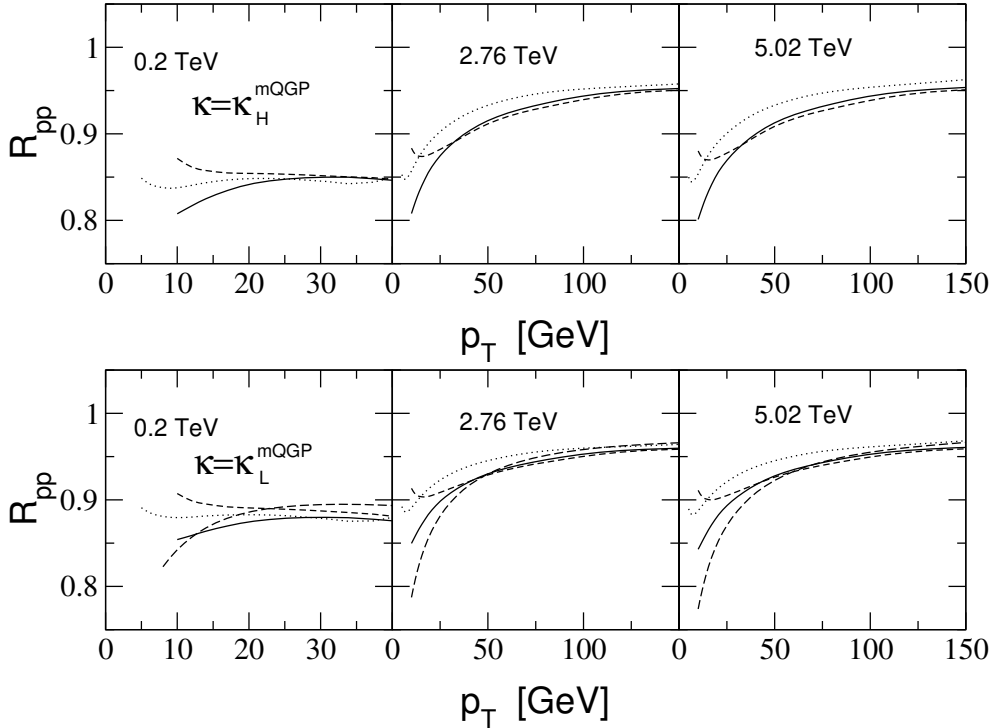


FIG. 1: R_{pp} of D mesons (solid), B mesons (dashed), and HFES (dotted) for 0.2, 2.76, and 5.02 TeV pp collisions. In the upper(lower) panels the curves are for $\kappa = \kappa_H^{\text{mQGP}}$ (κ_L^{mQGP}). In the lower panels we also plot R_{pp} for charged hadrons (long-dashed).

the medium effects for heavy flavors and light hadrons, in the lower panels we also plot R_{pp} for charged hadrons. From Fig. 1 one can see that the difference between the heavy flavor R_{pp} at the LHC energies for the L and H versions of the parameter κ becomes small at $p_T \gtrsim 30$ GeV. And at $p_T \sim 10 - 20$ GeV for the optimal values κ_H (κ_H^{mQGP}) heavy flavors the quantity $|R_{pp} - 1|$ are larger than those for κ_L (κ_L^{mQGP}) by $\sim 20 - 25\%$. As one can see from Fig. 1, for the LHC energies R_{pp} for heavy mesons and light hadrons become similar at $p_T \gtrsim 30$ GeV.

In Fig. 2 we compare our results for R_{AA} of D mesons with the LHC data from ALICE [57] for 2.76 TeV Pb+Pb collisions. We show the curves for the scenarios with (solid) and without (dashed) mQGP formation in pp collisions for the optimal values of κ obtained from the LHC data on heavy flavor R_{AA} (thick lines) and from R_{AA} of light hadrons (thin lines). In Fig. 3 we show comparison of our results for R_{AA} of D and B mesons for 5.02 TeV Pb+Pb collisions with data from ALICE [59] and CMS [60, 63]. The results for R_{AA} of D mesons shown in figures 2 and 3 are sensitive to the charm quark energy loss. We also calculated R_{AA} for D mesons from B hadron decays (nonprompt D), which is sensitive to the bottom quark energy loss. Figure 4 shows the comparison of our results for R_{AA} of nonprompt D mesons in 5.02 TeV Pb+Pb collisions with data from ALICE [64] and CMS [65]. In Fig. 5 we compare results for the ratio $R_{AA}^{\text{nonprompt}}/R_{AA}^{\text{prompt}}$ with data from ALICE [64]. From Figs. 3–5 one can see that the model describes reasonably the difference in the strength of jet quenching for the prompt and nonprompt D mesons (which is sensitive to the mass dependence of the quark energy loss). In Figs. 6 and 7 we compare our results for R_{AA} of HFES in 2.76 and 5.02 TeV Pb+Pb collisions with data from ALICE [61, 62]. These figures correspond to nuclear suppression of the total HFE spectrum that includes $c \rightarrow e$ and $b \rightarrow e$ decays. Figure 8 shows comparison of our calculations of R_{AA} for $b \rightarrow e$ and $c \rightarrow e$ channels separately with data from ALICE [66] for the $b \rightarrow e$ channel and with the results of analysis [67] within a data-driven method of charm and beauty isolation.

From Figs. 2–8 one can see that the difference between theoretical R_{AA} for D and B mesons, and HFES for scenarios with and without the mQGP formation in pp collisions is small. One can see that

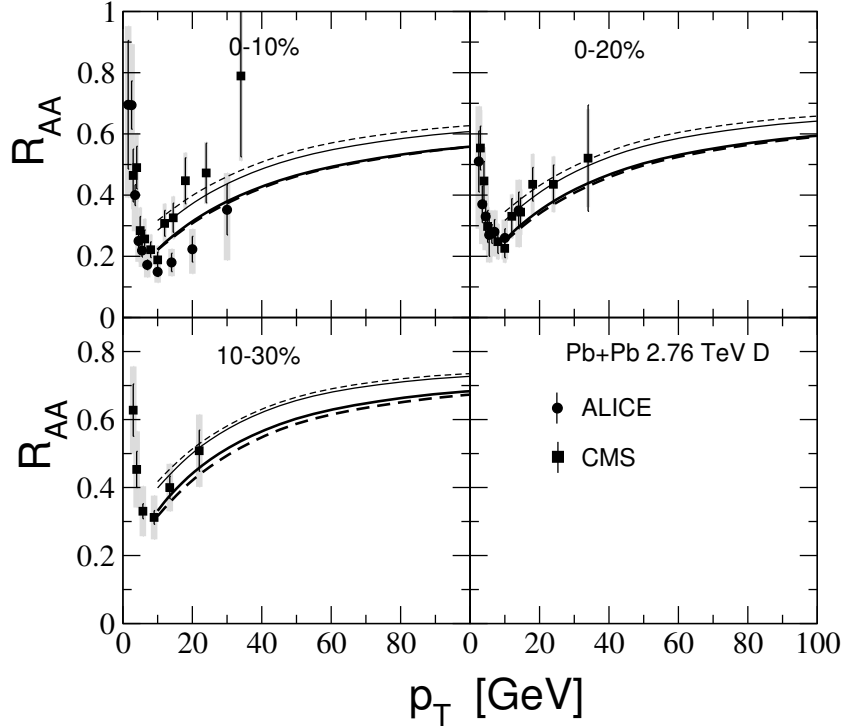


FIG. 2: R_{AA} of D mesons for 2.76 TeV Pb+Pb collisions from our calculations for scenarios with (solid) and without (dashed) mQGP formation in pp collisions for the optimal parameters $\kappa_H^{mQGP}(\kappa_H)$ (thick lines) and $\kappa_L^{mQGP}(\kappa_L)$ (thin lines). Data points are from ALICE [57] and CMS [58].

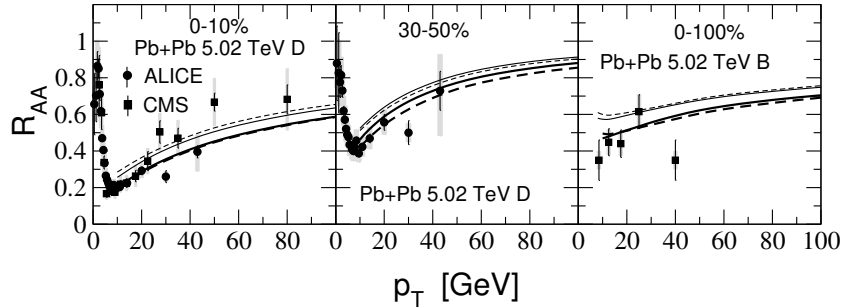


FIG. 3: R_{AA} of D mesons (left and middle plots) and B mesons (right plot) for 5.02 TeV Pb+Pb collisions. Curves are as in Fig. 2. Data points for D mesons are from ALICE [59] and CMS [60], and for B mesons from CMS [63].

both for $\kappa_H(\kappa_H^{mQGP})$ and $\kappa_L(\kappa_L^{mQGP})$ the results show reasonable agreement with experimental data. Note that the results shown in Figs. 3–5 and 8 demonstrate that the model reproduces reasonably the relative strength of jet quenching for charm and bottom quarks (i.e. the model reproduces reasonably the quark mass effects).

In Fig. 9 we compare our results for v_2 of prompt and nonprompt D mesons in 5.02 TeV Pb+Pb collisions to data from ALICE [68] and CMS [69, 70]. Unfortunately, experimental errors are too large to make a conclusive statement on agreement with the data. From Fig. 9 one sees that the relative effect of the mQGP formation in pp collisions on the theoretical predictions for v_2 is more pronounced than for R_{AA} . This occurs because the scenario with the mQGP formation in pp collisions requires somewhat stronger jet quenching for particle spectra than that without the mQGP formation in pp collisions (to

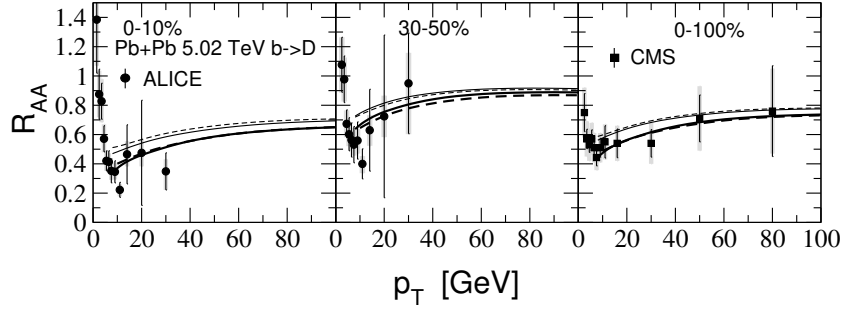


FIG. 4: R_{AA} of nonprompt D mesons from $B \rightarrow D^0$ decays. Curves are as in Fig. 2. Data points are from ALICE [64] and CMS [65].

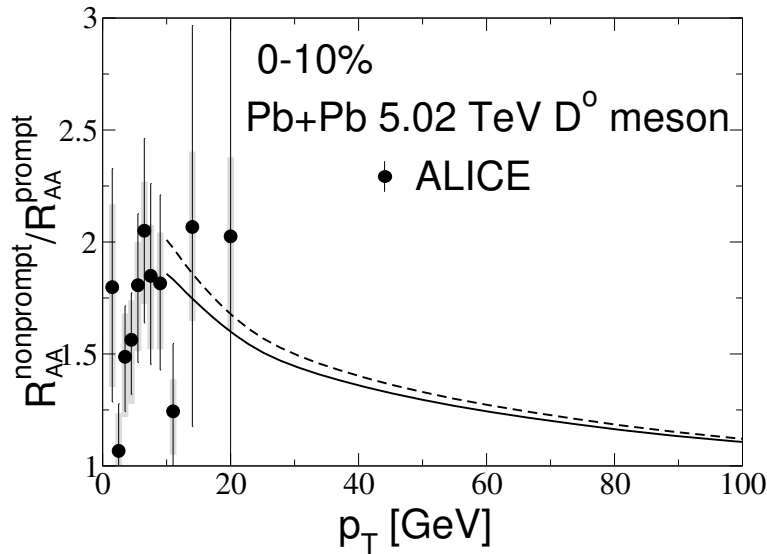


FIG. 5: Nonprompt to prompt D^0 -meson R_{AA} ratio vs p_T in the 0–10% central 5.02 TeV Pb+Pb collisions from our calculations for scenarios with (solid) and without (dashed) mQGP formation in pp collisions for the optimal parameters κ_H^{mQGP} and κ_H . Data points are from ALICE [64].

compensate the effect of the $1/R_{pp}$ factor on R_{AA}). As a consequence, for scenario with the mQGP formation we have a larger azimuthal anisotropy v_2 , which is not affected by the $1/R_{pp}$ factor.

In Fig. 10 we compare our results for R_{AA} of D mesons in 0.2 TeV Au+Au collisions to data from STAR [71]. In this figure, in addition to the scenarios with and without mQGP formation in pp collisions, we also present predictions for an intermediate scenario, in which the mQGP production in pp collisions occurs only at the LHC energies. In this scenario R_{AA} for 0.2 TeV Au+Au collisions should be calculated without $1/R_{pp}$ factor for the optimal κ fixed from the LHC data on R_{AA} for the scenario with the mQGP production in pp collisions (i.e., for $\kappa = \kappa_{L,H}^{mQGP}$). Unfortunately, the STAR data [71] are restricted to rather low transverse momenta, where the applicability of our model may be questionable. From Fig. 10 one can see that, for the maximal transverse momentum ($p_T \sim 8$ GeV) in the STAR data, our results, within errors, are consistent with the experimental data. We get a somewhat better agreement with the data for the intermediate scenario with the mQGP formation in pp collisions only at the LHC energies.

In Fig. 11 we compare our predictions for R_{AA} of the HFES for $b + c \rightarrow e$ decays in 0.2 TeV Au+Au collisions to RHIC data from STAR [24] and PHENIX [72]. Figure 12 shows comparison to data on R_{AA} from STAR [73] for the total ($b + c \rightarrow e$) electron spectrum and separately for $b \rightarrow e$ and $c \rightarrow e$ channels. From Figs. 11 and 12 one can see that for R_{AA} of HFES, as in the case of the results for R_{AA} of D

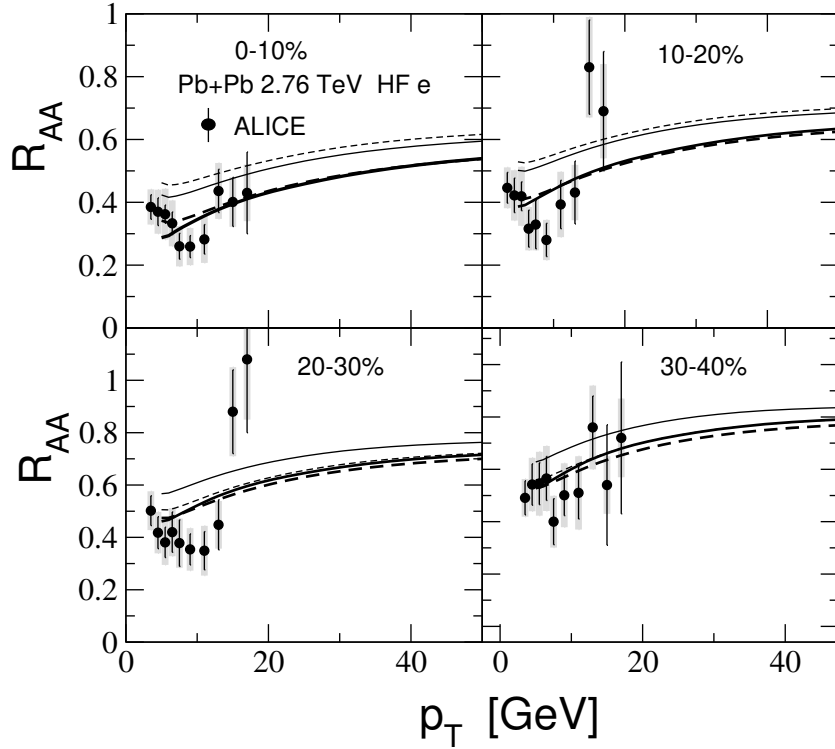


FIG. 6: Same as in Fig. 2 for HFEs at $\sqrt{s} = 2.76$ TeV. Data points are from ALICE [61].

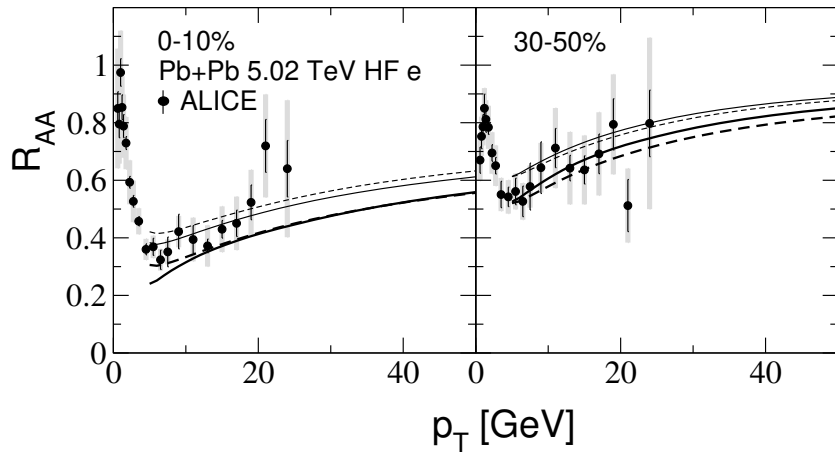


FIG. 7: Same as in Fig. 6 for $\sqrt{s} = 5.02$ TeV. Data points are from ALICE [62].

mesons shown in Fig. 10, the agreement with the experimental data becomes somewhat better for the intermediate scenario with the mQGP formation in pp collisions only at the LHC energies. However, a definite conclusion cannot be drawn given large experimental errors and a very restricted p_T range ($p_T \lesssim 8$ GeV) of the data.

Thus, from Figs. 2–12 we can conclude that altogether our theoretical results for scenarios with and without mQGP formation in pp collisions agree reasonably with experimental data on jet quenching for heavy flavors. However, our fits to heavy flavor R_{AA} give smaller values of κ than those for light hadrons, i.e. heavy flavor jet quenching data require somewhat bigger α_s than data on jet quenching for light

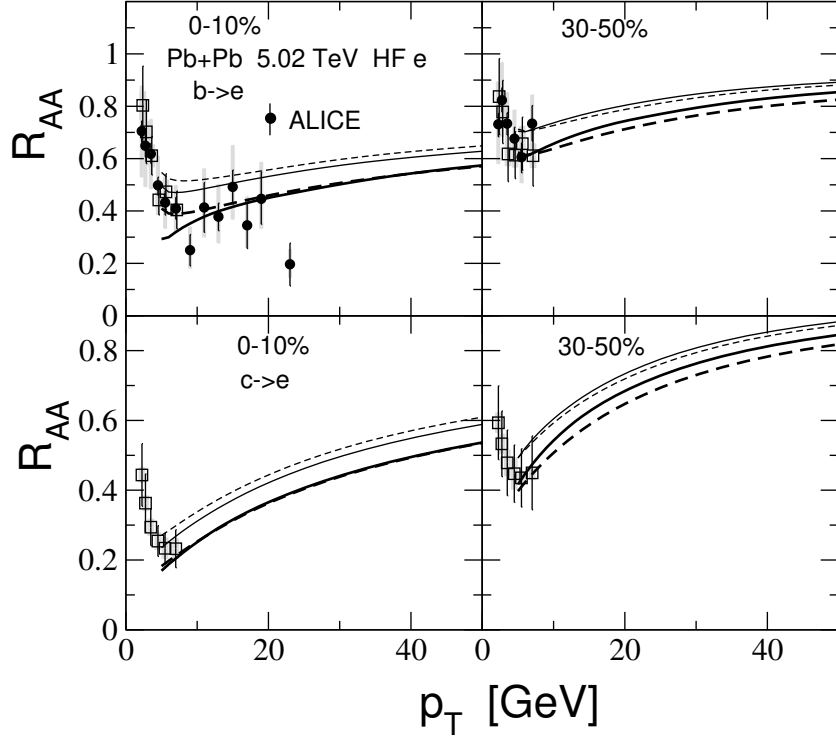


FIG. 8: R_{AA} of electrons from bottom (upper part) and charm (lower part) quark decays in Pb+Pb collisions at $\sqrt{s} = 5.02$ TeV. Curves are as in Fig. 2. Data points are from ALICE [66] (circles) and from the analysis by D. Li *et al.* [67] (squares) within a data-driven method of charm and bottom quark isolation.

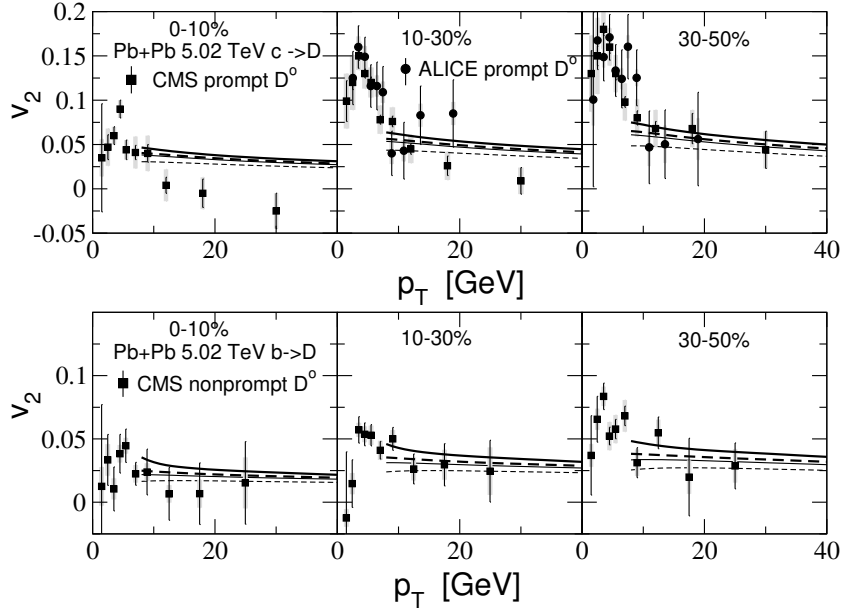


FIG. 9: v_2 for prompt (upper) and nonprompt (lower) D mesons in 5.02 TeV Pb+Pb collisions. Curves are as in Fig. 2. Data points are from ALICE [68] and CMS [69, 70].

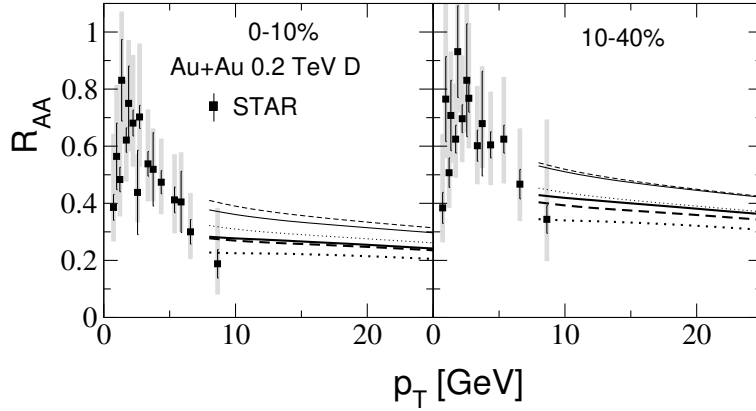


FIG. 10: R_{AA} of D^0 mesons in Au+Au collisions at $\sqrt{s} = 200$ GeV for 0–10% (left) and 10–40% (right) centrality bins. The solid and dashed lines are same as in Fig. 2. The dotted lines show results for scenario without mQGP formation in pp collisions obtained with parameters κ_L^{mQGP} (thin lines) and κ_H^{mQGP} (thick lines). Data points are from STAR [71].

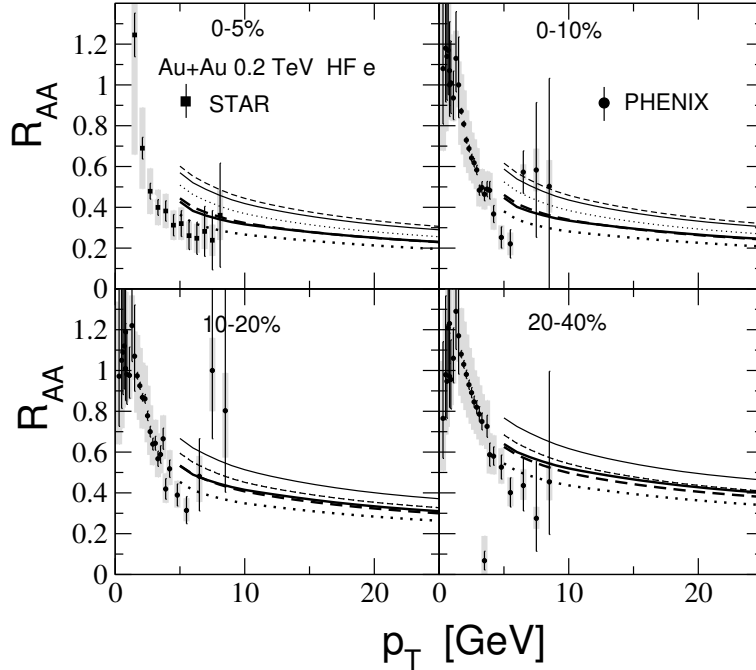


FIG. 11: Same as in Fig. 10 for HFEs. Data points are from STAR [24] and PHENIX [72].

hadrons. This inconsistency could be due to the approximations used in calculations of R_{AA} from the one gluon emission spectrum. One of the possible reasons is the use of the approximation of independent gluon emission [50] for the multiple gluon radiation. One can expect that this approximation becomes less reliable for gluons. Since at the LHC energies the gluon contribution to the high- p_T light hadron spectrum is large, it is clear that the different levels of inaccuracy of this approximation for quarks and gluons can lead to an inconsistency in the optimal values of κ fitted to data on R_{AA} for heavy flavors and light hadrons. Also, some inconsistency between the optimal κ for heavy flavors and light hadrons, may arise due to the approximation of a flat fireball density, because this approximation may somewhat overestimate the effect of the boundary gluon emission which becomes stronger for gluons.

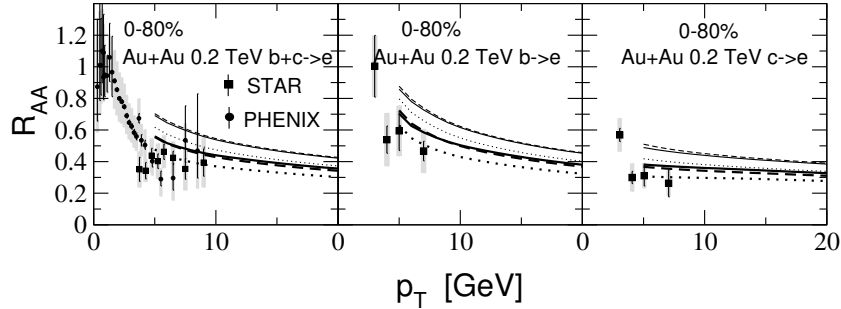


FIG. 12: The HFE R_{AA} in Au+Au collisions at $\sqrt{s} = 0.2$ TeV for minimum-bias centrality 0–80% interval. (left) The inclusive $b + c \rightarrow e$ R_{AA} . (middle) R_{AA} for bottom-decay electrons. (right) R_{AA} for charm-decay electrons. Curves are as in Fig. 10. Data points are from PHENIX [72] and STAR [73].

IV. SUMMARY

In this paper we presented results of a global analysis of experimental data on jet quenching for heavy flavors (for D , B mesons, and HFEs) within the LCPI [2] approach to induced gluon emission for scenarios with and without mQGP formation in pp collisions. The present analysis extends to heavy flavors our previous jet quenching analysis for light hadrons [19]. As in [19], we perform calculations for a temperature dependent running coupling $\alpha_s(Q, T)$, which has a plateau around $Q \sim Q_{fr} = \kappa T$. This parametrization is motivated by the lattice calculation [20] of the in-medium QCD coupling in the QGP. We performed calculations for two sets of the optimal values of the parameter κ . For the first set we use κ fitted to the LHC data on the heavy flavor R_{AA} in 2.76 and 5.02 TeV Pb+Pb collisions, and for the second set we use κ fitted to the LHC data on R_{AA} of light hadrons in 2.76 and 5.02 TeV Pb+Pb, and 5.44 TeV Xe+Xe collisions. We find that fits to heavy flavor R_{AA} give smaller values of κ than those for light hadrons, i.e. heavy flavor jet quenching data require somewhat bigger α_s than data on jet quenching for light hadrons. But the difference in the quality of agreement of the theoretical results with experimental data for heavy flavors for two sets of κ is not significant.

We find that the theoretical predictions for the nuclear modification factor R_{AA} for heavy flavors at the LHC energies for scenarios with and without mQGP formation in pp collisions are very similar, but the effect of the mQGP formation in pp collisions on predictions for azimuthal asymmetry v_2 is more pronounced. The results for R_{AA} and v_2 agree reasonably with the LHC data both for κ fitted to R_{AA} for heavy flavor and R_{AA} for light hadrons. The model reproduces reasonably the experimental relative strength of jet quenching for charm and bottom quarks (i.e. it reproduces reasonably the quark mass effects).

Note that, similarly to results of our analysis of jet quenching for light hadrons [19], from comparison with the RHIC data on R_{AA} of D mesons and of HFEs, we find that the agreement with data at the RHIC energies becomes somewhat better for the intermediate scenario, in which the mQGP formation in pp collisions occurs only at the LHC energies. This is also supported by our analysis [18] of the data from ALICE [17] on the UE multiplicity dependence of the medium modification factor I_{pp} .

Acknowledgements

This work is supported by the State program 0033-2019-0005.

Appendix

In this appendix we give, for the convenience of the reader, formulas for calculation of the gluon emission x -spectrum dP/dx . We use the representation of the induced gluon spectrum obtained in Ref. [31] with the prescription of [74] for incorporating the T -dependent running α_s . For a fast quark with momentum

along the z -axis produced at $z = 0$ in the matter of thickness L , dP/dx has the form

$$\frac{dP}{dx} = \int_0^L dz n(z) \frac{d\sigma_{eff}^{BH}(x, z)}{dx}, \quad (11)$$

where $n(z)$ is the medium number density, $d\sigma_{eff}^{BH}/dx$ is an effective Bethe-Heitler cross section for $q \rightarrow gq$ process, given by

$$\begin{aligned} \frac{d\sigma_{eff}^{BH}(x, z)}{dx} = & -\frac{P_q^g(x)}{\pi M} \text{Im} \int_0^z d\xi \sqrt{\alpha_s(Q(\xi), T(z-\xi))\alpha_s(Q(\xi), T(z+\xi))} \\ & \times \exp\left(-i\frac{\xi}{L_f}\right) \frac{\partial}{\partial \rho} \left(\frac{F(\xi, \rho)}{\sqrt{\rho}}\right) \Big|_{\rho=0}. \end{aligned} \quad (12)$$

Here $P_q^g(x) = (4/3)[1 + (1-x)^2]/x$ is the ordinary pQCD $q \rightarrow g$ splitting function, $M = E_q x(1-x)$, $L_f = 2M/\epsilon^2$, $\epsilon^2 = m_q^2 x^2 + m_{\bar{q}}^2(1-x)$, $Q^2(\xi) = aM/\xi$ with $a \approx 1.85$ [8], F is the solution to the radial Schrödinger equation

$$i\frac{\partial F(\xi, \rho)}{\partial \xi} = \left[-\frac{1}{2M} \left(\frac{\partial}{\partial \rho}\right)^2 + v(\rho, x, z-\xi) + \frac{4m^2-1}{8M\rho^2} \right] F(\xi, \rho) \quad (13)$$

with the azimuthal quantum number $m = 1$, and the boundary condition $F(\xi = 0, \rho) = \sqrt{\rho}\sigma_{gq\bar{q}}(\rho, x, z)\epsilon K_1(\epsilon\rho)$ at $\xi = 0$ (K_1 is the Bessel function). The potential v reads

$$v(\rho, x, z) = -i\frac{n(z)\sigma_{gq\bar{q}}(\rho, x, z)}{2}, \quad (14)$$

where $\sigma_{gq\bar{q}}(\rho, x, z)$ is the three-body cross section of interaction of the $gq\bar{q}$ system with a medium constituent located at z (ρ is the transverse distance between g and the final quark q). In the transverse plane \bar{q} is located at the center of mass of the gq pair. The $\sigma_{gq\bar{q}}$ can be written via the local dipole cross section $\sigma_{q\bar{q}}(\rho, z)$ (for the color singlet $q\bar{q}$ pair)

$$\sigma_{gq\bar{q}}(\rho, x, z)|_{q \rightarrow gq} = \frac{9}{8}[\sigma_{q\bar{q}}(\rho, z) + \sigma_{q\bar{q}}((1-x)\rho, z)] - \frac{1}{8}\sigma_{q\bar{q}}(x\rho, z). \quad (15)$$

In the two-gluon approximation the dipole cross section reads

$$\sigma_{q\bar{q}}(\rho, z) = C_T C_F \int d\mathbf{q} \alpha_s^2(q, T(z)) \frac{[1 - \exp(i\mathbf{q}\boldsymbol{\rho})]}{[q^2 + \mu_D^2(z)]^2}, \quad (16)$$

where $C_{F,T}$ are the color Casimir for the quark and thermal parton (quark or gluon), and $\mu_D(z)$ is the local Debye mass.

For the QGP fireball in AA collisions the coordinate z coincides with the proper time τ , i.e. in terms of the real fireball number density, $n_f(\boldsymbol{\rho}, \tau)$, we have $n(z) = n_f(\boldsymbol{\rho}_j(\boldsymbol{\rho}_{j0}, \tau), \tau)$, where $\boldsymbol{\rho}_{j0}$ is the jet production transverse coordinate, and $\boldsymbol{\rho}_j(\boldsymbol{\rho}_{j0}, \tau) = \boldsymbol{\rho}_{j0} + \tau\mathbf{p}_T/|\mathbf{p}_T|$ is the jet trajectory. We use the approximation of a uniform fireball. In this case, inside the fireball, the function $n_f(\boldsymbol{\rho}, \tau)$ does not depend on the jet production point. This greatly reduces the computational cost, since one can tabulate the L -dependence of the induced gluon spectrum once, and then use it for calculations of the FFs for arbitrary jet geometry.

[1] R. Baier, Y.L. Dokshitzer, A.H. Mueller, S. Peigné, and D. Schiff, Nucl. Phys. B**483**, 291 (1997) [arXiv:hep-ph/9607355].

- [2] B.G. Zakharov, JETP Lett. **63**, 952 (1996) [arXiv:hep-ph/9607440].
- [3] U.A. Wiedemann, Nucl. Phys. **A690**, 731 (2001) [arXiv:hep-ph/0008241].
- [4] M. Gyulassy, P. Lévai, and I. Vitev, Nucl. Phys. **B594**, 371 (2001) [arXiv:hep-ph/0006010].
- [5] P. Arnold, G.D. Moore, and L.G. Yaffe, JHEP **0206**, 030 (2002) [arXiv:hep-ph/0204343].
- [6] R. Baier, D. Schiff, and B.G. Zakharov, Ann. Rev. Nucl. Part. Sci. **50**, 37 (2000) [arXiv:hep-ph/0002198].
- [7] J.D. Bjorken, Fermilab preprint 82/59-THY (1982, unpublished).
- [8] B.G. Zakharov, JETP Lett. **86**, 444 (2007) [arXiv:0708.0816].
- [9] W. Broniowski and W. Florkowski, Phys. Rev. **C65**, 024905 (2002) [arXiv:nucl-th/0110020].
- [10] V. Khachatryan *et al.* [CMS Collaboration], JHEP **1009**, 091 (2010) [arXiv:1009.4122].
- [11] G. Aad *et al.* [ATLAS Collaboration], Phys. Rev. Lett. **116**, 172301 (2016) [arXiv:1509.04776].
- [12] J. Adam *et al.* [ALICE Collaboration], Nature Phys. **13**, 535 (2017) [arXiv:1606.07424].
- [13] R. Campanini, G. Ferri, and G. Ferri, Phys. Lett. **B703**, 237 (2011), [arXiv:1106.2008].
- [14] L. Van Hove, Phys. Lett. **B118**, 138 (1982).
- [15] R. Field, Acta Phys. Polon. **B42**, 2631 (2011) [arXiv:1110.5530].
- [16] B.G. Zakharov, Phys. Rev. Lett. **112**, 032301 (2014) [arXiv:1307.3674].
- [17] S. Tripathy [for ALICE Collaboration], arXiv:2103.07218.
- [18] B.G. Zakharov, JETP Lett. **116**, 347 (2022) [arXiv:2208.10339].
- [19] B.G. Zakharov, JHEP **09**, 087 (2021) [arXiv:2105.09350].
- [20] A. Bazavov *et al.*, Phys. Rev. **D98**, 054511 (2018) [arXiv:1804.10600].
- [21] J. Braun and H. Gies, Phys. Lett. **B645**, 53 (2007) [arXiv:hep-ph/0512085].
- [22] L. Apolinário, Y.-J. Lee, and M. Winn, Prog. Part. Nucl. Phys. **127**, 103990 (2022) [arXiv:2203.16352].
- [23] Y.L. Dokshitzer and D.E. Kharzeev, Phys. Lett. **B519**, 199 (2001) [arXiv:hep-ph/0106202].
- [24] B.I. Abelev *et al.* [STAR Collaboration], Phys. Rev. Lett. **98**, 192301 (2007) , Erratum-ibid. 106 (2011) 159902 [arXiv:nucl-ex/0607012].
- [25] S.S. Adler *et al.* [PHENIX Collaboration], Phys. Rev. Lett. **96**, 032301 (2006).
- [26] P. Aurenche and B.G. Zakharov, JETP Lett. **90**, 237 (2009) [arXiv:0907.1918].
- [27] B.G. Zakharov, JETP Lett. **96**, 616 (2013) [arXiv:1210.4148].
- [28] B.G. Zakharov, J. Phys. **G40**, 085003 (2013) [arXiv:1304.5742].
- [29] B.G. Zakharov, JETP Lett. **103**, 363 (2016) [arXiv:1509.07020].
- [30] B.G. Zakharov, JETP **129**, 521 (2019) [arXiv:1912.04875].
- [31] B.G. Zakharov, JETP Lett. **80**, 617 (2004) [arXiv:hep-ph/0410321].
- [32] S. Shi, J. Liao, M. Gyulassy, Chin. Phys. **C43**, 044101 (2019) [arXiv:1808.05461].
- [33] D. Zigic, B. Ilic, Marko Djordjevic and Magdalena Djordjevic, Phys. Rev. **C101**, 064909 (2020) [arXiv:1908.11866].
- [34] B. Blok and K. Tywoniuk, Eur. Phys. J. **C79**, 560 (2019) [arXiv:1901.07864].
- [35] B. Blok, Eur. Phys. J. **C80**, 729 (2020) [arXiv:2002.11233].
- [36] B. Blok, Eur. Phys. J. **C81**, 832 (2021) [arXiv:2009.00465].
- [37] R. Rapp, P.B. Gossiaux, A. Andronic, R. Auerbeck, S. Masciocchi, A. Beraudo, E. Bratkovskaya, P. Braun-Munzinger, S. Cao, A. Dainese, S.K. Das, M. Djordjevic, V. Greco, M. He, H. van Hees, G. Inghirami, O. Kaczmarek, Y.-J. Lee, J. Liao, S.Y.F. Liu, G. Moore, M. Nahrgang, J. Pawlowski, P. Petreczky, S. Plumari, F. Prino, S. Shi, T. Song, J. Stachel, I. Vitev, and X.-N. Wang, Nucl. Phys. **A979**, 21 (2018) [arXiv:1803.03824].
- [38] Zhong-Bo Kang, F. Ringer, and I. Vitev, JHEP **03**, 146 (2017) [arXiv:1610.02043].
- [39] P. Lévai and U. Heinz, Phys. Rev. **C57**, 1879 (1998) [arXiv:hep-ph/9710463].
- [40] B.G. Zakharov, JETP Lett. **88**, 781 (2008) [arXiv:0811.0445].
- [41] B.G. Zakharov, J. Phys. **G48**, 055009 (2021) [arXiv:2007.09772].
- [42] S. Kretzer, H.L. Lai, F. Olness, and W.K. Tung, Phys. Rev. **D69**, 114005 (2004) [arXiv:hep-ph/0307022].
- [43] K.J. Eskola, H. Paukkunen, and C.A. Salgado, JHEP **0904**, 065 (2009) [arXiv:0902.4154].
- [44] T. Sjostrand, L. Lonnblad, S. Mrenna, and P. Skands, arXiv:hep-ph/0308153.
- [45] M. Cacciari, P. Nason, and R. Vogt, Phys. Rev. Lett. **95**, 122001 (2005).
- [46] A.H. Mahmood *et al.* [CLEO Collaboration], Phys. Rev. **D70**, 032003 (2004).
- [47] R. Poling, invited talk at 4th Flavor Physics and CP Violation Conference, Vancouver, British Columbia, Canada, 9-12 Apr 2006, arXiv:hep-ex/0606016.
- [48] B. Aubert *et al.* [BaBar Collaboration], Phys. Rev. **D75**, 072002 (2007) [arXiv:hep-ex/0606026].
- [49] O. Kaczmarek and F. Zantow, Phys. Rev. **D71**, 114510 (2005) [arXiv:hep-lat/0503017].
- [50] R. Baier, Y.L. Dokshitzer, A.H. Mueller, and D. Schiff, JHEP **0109**, 033 (2001) [arXiv:hep-ph/0106347].
- [51] J.D. Bjorken, Phys. Rev. **D27**, 140 (1983).
- [52] D. Kharzeev and M. Nardi, Phys. Lett. **B507**, 121 (2001) [arXiv:nucl-th/0012025].
- [53] B.G. Zakharov, JETP **124**, 860 (2017) [arXiv:1611.05825].
- [54] B.G. Zakharov, Eur. Phys. J. **C78**, 427 (2018) [arXiv:1804.05405].
- [55] B. Müller and K. Rajagopal, Eur. Phys. J. **C43**, 15 (2005) [arXiv:hep-ph/0502174].
- [56] S. Borsanyi, G. Endrodi, Z. Fodor, A. Jakovac, S.D. Katz, S. Krieg, C. Ratti, and K. K. Szabo, JHEP **1011**,

- 077 (2010) [arXiv:1007.2580].
- [57] . J. Adam *et al.* [ALICE Collaboration], JHEP **03**, 081 (2016) [arXiv:1509.06888].
 - [58] Nuclear Modification Factor of prompt D^0 in PbPb Collisions at $\sqrt{s_{NN}} = 2.76$ TeV, 2015 Tech. Rep. CMS-PAS-HIN-15-005 CERN Geneva URL <https://cds.cern.ch/record/2055466/files/HIN-15-005-pas.pdf>
 - [59] S. Acharya *et al.* [ALICE Collaboration], JHEP **01**, 174 (2022) [arXiv:2110.09420].
 - [60] A.M. Sirunyan *et al.* [CMS Collaboration], Phys. Lett. B**782**, 474 (2018) [arXiv:1708.04962].
 - [61] J. Adam *et al.* [ALICE Collaboration], Phys. Lett. B**771**, 467 (2017) [arXiv:1609.07104].
 - [62] S. Acharya *et al.* [ALICE Collaboration], Phys. Lett. B**804**, 135377 (2020) [arXiv:1910.09110].
 - [63] A.M. Sirunyan *et al.* [CMS Collaboration], Phys. Rev. Lett. **119**, 152301 (2017) [arXiv:1705.04727].
 - [64] S. Acharya *et al.* [ALICE Collaboration], 2202.00815.
 - [65] A.M. Sirunyan *et al.* [CMS Collaboration], Phys. Rev. Lett. **123**, 022001 (2019) [arXiv:1810.11102].
 - [66] J. Park, [for the ALICE Collaboration], 2021. Nuclear modification factor of electrons from open beauty-hadron decays in PbPb collisions at $\sqrt{s} = 5.02$ TeV with ALICE. PoS HardProbes2020, 034. doi:10.22323/1.387.0034.
 - [67] D. Li, F. Si, Y. Zhao, P. Zhou, Y. Zhang, X. Li, and C. Yang, Phys. Lett. B**832**, 137249 (2022) [arXiv:2110.08769].
 - [68] S. Acharya *et al.* [ALICE Collaboration], JHEP **02**, 150 (2019) [arXiv:1809.09371].
 - [69] A.M. Sirunyan *et al.* [CMS Collaboration], Phys. Lett. B**816**, 136253 (2021) [arXiv:2009.12628].
 - [70] Azimuthal anisotropy of nonprompt D^0 mesons in PbPb collisions at $\sqrt{s_{NN}} = 5.02$ TeV, 2021 Tech. Rep. CMS-PAS-HIN-21-003 CERN Geneva URL <https://cds.cern.ch/record/2806157/files/HIN-21-003-pas.pdf>.
 - [71] J. Adam *et al.* [STAR Collaboration], Phys. Rev. C**99**, 034908 (2019) [arXiv:1812.10224].
 - [72] A. Adare *et al.* [PHENIX Collaboration], Phys. Rev. C**84**, 044905 (2011) [arXiv:1005.1627].
 - [73] M.S. Abdallah *et al.* [STAR Collaboration], arXiv:2111.14615.
 - [74] B.G. Zakharov, JETP Lett. **112**, 681 (2020) [arXiv:2011.01526].